J Appl Electrochem (2009) 39:1–5
DOI 10.1007/s10800-008-9634-z

ORIGINAL PAPER

MnO_2 cathode in an aqueous Li_2SO_4 solution for battery applications

Manickam Minakshi · David R. G. Mitchell

Received: 22 February 2008 / Accepted: 23 June 2008 / Published online: 17 July 2008

Abstract A manganese dioxide (MnO_2) cathode with zinc (Zn) as the anode has been investigated using lithium sulphate (Li_2SO_4) as an electrolyte. Previously we demonstrated that cells comprising MnO_2 and lithium hydroxide (LiOH) as an electrolyte can be made rechargeable to over one-electron capacity with a discharge capacity of 150 mAh g^{-1}. Here we have extended our work to assess Li_2SO_4 as an electrolyte and have found that the battery is not rechargeable. Based on the electrochemical (discharge/charge) performance and the products formed following discharge and charge, the mechanism proposed for the sulphate-based media is one of proton insertion into the MnO_2 cathode, rather than the lithium ion insertion observed for the LiOH electrolyte. The addition of bismuth species to the Li_2SO_4-based cell results in a transition to rechargeable behaviour. This is believed to be due to the influence of Bi ions on the formation of soluble Mn^{3+} soluble intermediates. However, the coulombic efficiency of the cell diminishes rapidly with repeated charge/discharge cycles. This confirms that the nature of the Li-containing electrolyte has a marked influence on the electrochemistry of the cell.

Keywords Sulphate · Electrolyte · MnO_2 · Proton · XRD · SEM

M. Minakshi (✉)
Department of Extractive Metallurgy, Murdoch University, Murdoch, WA 6150, Australia
e-mail: minakshi@murdoch.edu.au;
lithiumbattery@hotmail.com

D. R. G. Mitchell
Institute of Materials and Engineering, ANSTO, PMB 1, Menai, NSW 2234, Australia

1 Introduction

Due to its high positive electrode potential, non-toxicity and low molecular weight, manganese dioxide (MnO_2) appears to be one of the most promising candidates as a cathode for the next generation of battery systems. It has found wide spread use as a cathode in Leclanche cells [1] and more recently in secondary batteries, in particular to lithium batteries [2, 3].

Since its introduction in the early 1960s, the Zn–MnO_2 aqueous battery using potassium hydroxide (KOH) as an electrolyte has dominated the primary battery market [4], predominantly due to their low cost and high capacity. The drawback of Zn–MnO_2 systems is their poor rechargeability, even at very shallow depths of discharge. Therefore this battery is limited to primary applications. Numerous attempts have made to overcome the lack of rechargeability of MnO_2 materials and to understand the redox mechanism involved in $Mn^{4+/2+}$ transitions. However, neither the reaction mechanisms, nor the persisting limitations of rechargeability are clearly understood. Until recently, batteries using a MnO_2 cathode and KOH as the electrolyte were effectively non-rechargeable [5–7]. In one of our recent reported works we demonstrated that cells comprising MnO_2 as a cathode and using lithium hydroxide as electrolyte can be made rechargeable over multiple discharge cycles [8]. This involves a lithium intercalation mechanism into the MnO_2 lattice. However, the cycling ability of this cell is limited to around 50 cycles after which the utilization of the active MnO_2 material becomes low [9]. This motivated us to attempt to enhance the battery capacity by investigating alternative electrolytes and also the influence of small amounts of additive to the MnO_2. It is widely reported in the literature that foreign cations i.e. Pb^{4+} [10, 11] or Bi^{3+} [12, 13] stabilize the open birnessite

MnO_2 structure throughout the redox processes permitting greater depths of discharge/charge as well as greater capacity retention [14]. In the Bi-doped MnO_2/KOH cell Bi^{3+} ions have been found to minimize the magnitude of structural changes in the MnO_2 and thus enhance the rechargeability.

Aqueous rechargeable batteries are one of the promising candidates for energy storage in terms of safety and cost. Therefore, in this paper, we have extended our work in investigating the MnO_2 cathode in Li_2SO_4 aqueous electrolyte and also the influence of bismuth additions. Electrochemical properties were determined and the materials formed on the discharged/charged product were analysed by X-ray diffraction (XRD) and Fourier transform—infra red spectroscopy (FT-IR) and scanning electron microscopy (SEM) analysis.

2 Experimental

The MnO_2 material was purchased from Sigma Aldrich. Zn foil (99.9%) from BDH chemicals; analytical reagent grade lithium hydroxide monohydrate ($LiOH \cdot H_2O$) from Sigma Chemicals and lithium sulfate ($Li_2SO_4 \cdot H_2O$) and zinc sulphate Heptahydrate ($ZnSO_4 \cdot 7H_2O$) from BDH and Ajax chemicals respectively were used in this study. Bismuth oxide (Bi_2O_3) was obtained from Aldrich chemical company.

The MnO_2 active material was first mixed with 15 wt% of carbon black (A-99 Asbury USA) and with 5 wt% of poly (vinylidene difluoride) (PVDF, Sigma Aldrich) as a binder and then pressed into a disc shape with a diameter of 12 mm. In the case of Bi-doped MnO_2, 10 wt% of Bi_2O_3 is included in the mixture while adjusting the weight of active MnO_2 material. An electrochemical test cell was constructed with the disk as the cathode, Zn metal as the anode and filter paper as the separator. The electrolyte was a saturated solution of lithium hydroxide containing 1 mol L^{-1} zinc sulphate or 1 M of lithium sulphate were dissolved in deionized water to prepare solutions of required concentrations. The cells were discharged/charged galvanostatically in ambient atmosphere at 0.5 mA cm^{-2} by using an EG & G Princeton Applied Research Potentiostat/Galvanostat model 273A, operated by model 270 software (EG&G). The cut off discharge and charge voltages were 1.0 and 2.0 V respectively.

For X-ray analysis a Siemens X-ray diffractometer using Philips Cu-Kα radiation was used. The surface analysis of the materials was conducted by using a scanning electron microscope (Philips Analytical XL series 20). The FT-IR (Fourier transform infrared spectroscopy) spectra were recorded by using a Nicolet Magna-IR spectrometer. For each sample an average of 16 scans were recorded.

3 Results and discussions

The galvanostatic discharge/charge experiments were carried out by discharging and charging the Zn–MnO_2 battery at a constant current density of 0.5 mA cm^{-2} with the cut-off voltages of 1.0 and 2.0 V respectively. The present work investigates the reversibility on cells using as a MnO_2 electrode with lithium sulphate as electrolyte. To compare the effect of replacing LiOH with Li_2SO_4 as the electrolyte in a Zn–MnO_2 cell, we have carried out discharge–charge cycles on two identical cells one containing 1 M of Li_2SO_4 and the other saturated LiOH aqueous solution. The best results have been achieved only for these electrolyte concentrations.

The results for the first cycle for both the cells are shown in Fig. 1. It can be seen that the discharge curve for the cell with Li_2SO_4 is quite different from that of the LiOH cell (Fig. 1). Although, the cathode utilization for both the cells appears to be identical at 140 mAh g^{-1} for a given cut-off voltage of 1 V for both the cells, the voltage profiles are very different. Despite the close similarities in the open-circuit voltage (OCV) of 1.75 and 1.83 V for Li_2SO_4 and LiOH cells respectively (lithium-containing electrolytes are good ionic conductors, hence the high OCV), the two cells deviate from the outset of the discharge process. The decrease in cell potential was higher when Li_2SO_4 was the electrolyte. Below 1.3 V, the drop in potential was not smooth which indicates that the $Mn^{4+/2+}$ transitions are impeded. This could be due to hydrogen evolution [15]. In an aqueous electrolyte system, the hydrogen evolution occurs on the negative electrode after proton/lithium ion intercalation during discharge and oxygen is evolved on the positive electrode after extraction of lithium during the charge process. These evolution potentials critically depend on the pH of the aqueous solution [15]. However,

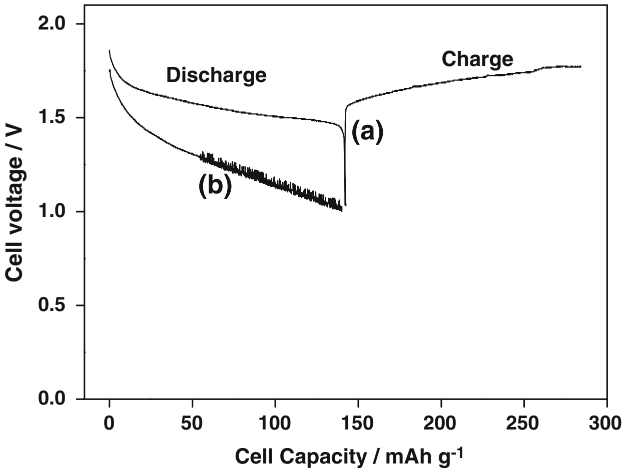

Fig. 1 The first discharge–charge behavior of MnO_2 cathode in: (**a**) saturated LiOH electrolyte and (**b**) 1 M Li_2SO_4 electrolyte

the hydrogen evolution can be effectively suppressed when a suitable additive is added [16].

For the LiOH cell, a flat mid discharge voltage from 1.6 down to 1.5 V was observed. This was followed by a sharp fall at 1.0 V. The sharp drop in potential in the LiOH-containing cell could be due to anodic failure. The flat discharge voltage region at ≈1.5 V corresponds to the $Mn^{4+/3+}$ redox reactions [17], and this was not observed in the Li_2SO_4-containing cell. This is clear evidence that the discharge mechanism is different between the two electrolytes.

On recharging, the process is reversible for the LiOH-containing cell with a coulombic efficiency of 92%. The Li_2SO_4–containing cell was unable to be recharged. One possible contributory factor to this difference in behaviour, is the formation of lithium carbonate (Li_2CO_3) in the LiOH-containing cell in the presence of atmospheric CO_2 (which is not excluded in the experiment). This layer coats the MnO_2 particles and may act as a barrier for protons while permitting lithium ion insertion in LiOH electrolyte forming lithium intercalated MnO_2 [8]. The carbonate layer does not form in the Li_2SO_4 electrolyte, so protons diffuse into MnO_2 with a low voltage profile while forming a non-rechargeable product of manganese oxy hydroxides.

To further understand the discharge mechanism, a small amount of Bi_2O_3 was added to MnO_2 cathode of the Li_2SO_4-containing cell. The presence of bismuth prevents the formation of non-rechargeable product (Mn_3O_4) [12, 13], which is the main cause of irreversibility of MnO_2. The first and tenth discharge-charge voltage profiles of the Bi-doped Li_2SO_4-containing cell are shown in Fig. 2. The Bi-doped MnO_2 (Fig. 2) showed a slightly higher discharge capacity of 165 mAh g^{-1} than the Bi-free Li_2SO_4-containing cell (140 mAh g^{-1}) (Fig. 1). The observed difference could be attributed to the presence of bismuth [14]. Importantly, the Bi additions made the Li_2SO_4-containing cell rechargeable. The shape of the charge curve is different to the discharge curve. The gradual downward sloping potential during discharge contrasted with a charge curve with a marked discontinuity between 1.5 and 1.75 V (Fig. 2). This plateau indicates that charging occurs in a two stage process, with the possible formation of a secondary phase. Although a large capacity loss was not observed in the subsequent cycles, capacity fade was present at the tenth cycle (Fig. 2). The capacity reduced by 30% from 165 to 115 mAh g^{-1}.

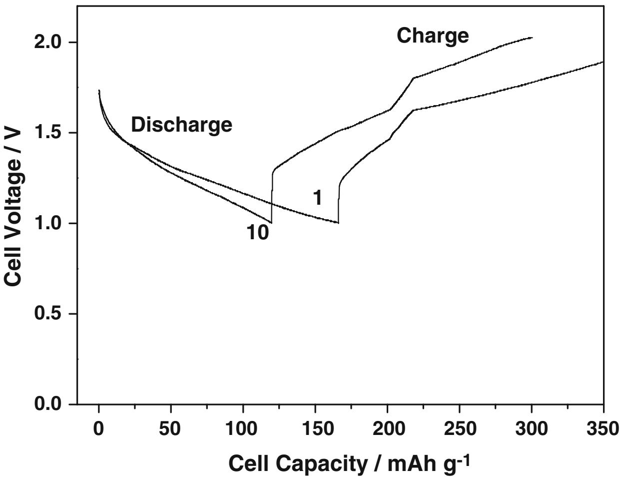

Fig. 2 The first and tenth discharge–charge behavior of Bi-doped MnO_2 cathode in a Li_2SO_4 electrolyte

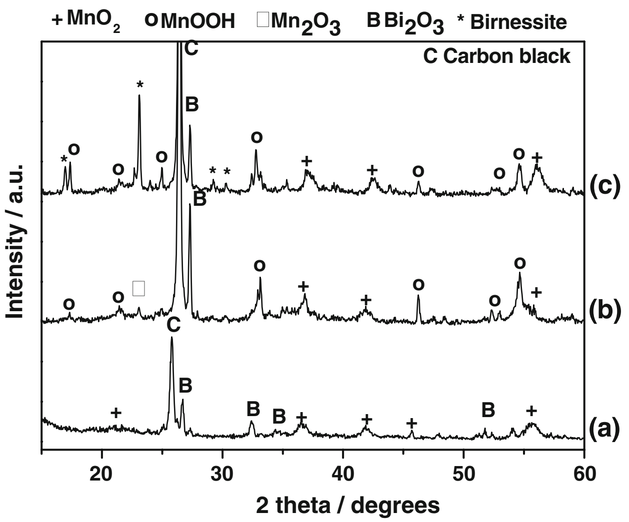

Fig. 3 XRD diffraction pattern of γ-MnO_2 mixed with Bi_2O_3 and AB (Acetylene black) and PVDF (binder) (**a**) before discharged (**b**) discharged and (**c**) charged after discharge in Li_2SO_4 electrolyte

The X-ray diffraction patterns shown in Fig. 3 are consistent with the electrochemical (discharge–charge) behavior in Fig. 2. Figure 3a shows the XRD pattern of the MnO_2 cathode doped with Bi_2O_3 before discharge. This material shows the characteristic peaks of MnO_2 (+) as indexed in the JCPDS data base (24-0735) in addition to the peaks corresponding to Bi_2O_3 (B) and a main Bragg reflection corresponding to graphite (acetylene black) (C). In the XRD pattern for the material after discharge in the Li_2SO_4-containing cell (Fig. 3b), MnOOH (O) appears to be the major product with a shoulder peak of Mn_2O_3 (□). The absence of the Mn_3O_4 (hausmannite) phase suggests that the presence of bismuth helps to suppress the formation of non-rechargeable product and made the cell rechargeable. The phases formed after recharge (Fig. 3c) have still retained the major peaks of MnOOH (O) while forming a well-developed crystalline birnessite (δ-MnO_2) (*). The results clearly demonstrate that the presence of bismuth helps to suppress the formation of Mn_3O_4 during discharge and helps the formation of a secondary phase, birnessite during charge with a distinct voltage plateaus (in

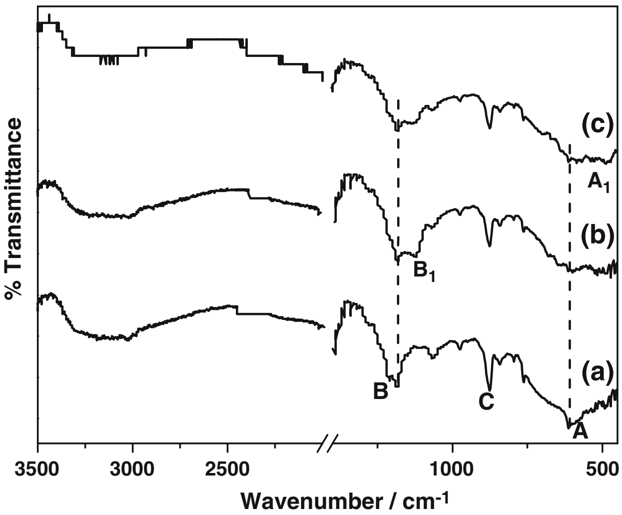

Fig. 4 Infra-red spectra of bismuth-doped MnO_2 cathode (**a**) before discharge (**b**) after discharge and (**c**) charged after discharge in Li_2SO_4 electrolyte

Fig. 2). Although the birnessite MnO_2 is an inactive material it does stabilizes the MnO_2 structure [18].

As suggested by Wroblowa et al. [12], the Bi^{3+} ions plays a critical role in maintaining open-layered structures of MnO_2 during the discharge–charge process. In order to view any changes in MnO_6 octahedra, during the discharge and charge processes, infra-red spectroscopy has been employed. Figure 4 shows the FT-IR spectra of MnO_2 before and after discharge and charged material in the Li_2SO_4-containing cell. Important spectral features in Fig. 4 are labelled A, B and C. The peak "A" in the region of 600 cm^{-1} is assigned to fundamental Mn–O vibrations in MnO_2 [19, 20]. The peaks "B" and "C" at 1200 and 875 cm^{-1} are attributed to the fundamental O–H bending mode. The broad peak in the higher wave numbers centred around 2700 and 3000 cm^{-1} is the fundamental O–H stretching band and absorbed water respectively. In the spectrum for the discharged material (Fig. 4b) and the same after charging (Fig. 4c) in Li_2SO_4-containing cell, additional peaks B_1 and A_1 are seen on discharged and charged samples respectively, compared with the as-prepared MnO_2 electrode (Fig. 4a). The peak at B_1 (Fig. 4b) is attributed to the OH-bending mode corresponding to δ-1-OH of MnOOH [21] and would suggest the formation of manganese oxy hydroxide (MnOOH) during discharge. This is consistent with the XRD analysis (Fig. 3b). The peak at A_1 in Fig. 4c is due to the birnessite MnO_2 phase formed during charging. The results obtained from the XRD and FT-IR spectroscopy show that the Bi^{3+} ions help to maintain the layered structures of both the discharged product (MnOOH) and the charged product (birnessite δ-MnO_2) a phase consisting of edge shared MnO_6 octahedra.

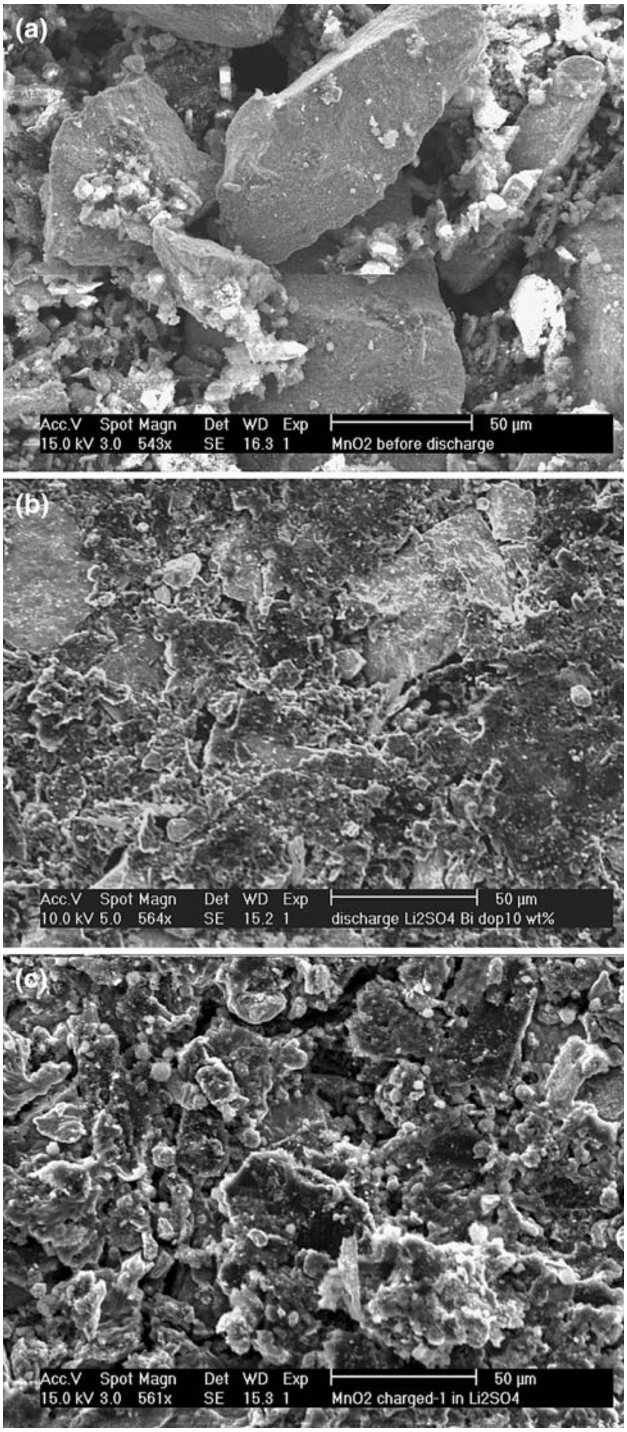

Fig. 5 SEM images of bismuth-doped MnO_2 cathodes (10 wt%) (**a**) before discharge (**b**) discharged and (**c**) charged samples. The shape and size of the primary MnO_2 particles appears to be changed by the discharged and charged processes

The surface morphology of the materials formed before and after discharge and its subsequent charge in Li_2SO_4-containing cell are compared in Fig. 5. The Bi-doped MnO_2 cathode before discharge (Fig. 5a) shows a well crystalline MnO_2 of particle size between 50 and 70 µms with Bi_2O_3 dispersed amongst it. For the same material after discharge, the morphology is quite different (Fig. 5b) with a layer of material coating the MnO_2 particles which XRD suggests this to be MnOOH (Fig. 3b). For the charged cathode (Fig. 5c), the smooth layer of MnOOH has transformed into more discrete particles, which may the birnessite phase detected with XRD (Fig. 3c). The coarse MnO_2 particles are present in all cases, since the Bi additions stabilise its structure.

These results support the view that a proton insertion mechanism operates in the Li_2SO_4-containing cell. Bi^{3+} ions clearly have a role in keeping the Mn^{3+} ions in the solution from dissolving to soluble Mn^{2+} thereby preventing the formation of unwanted discharge products like Mn_3O_4, $Mn(OH)_2$. In this regard, Li_2SO_4 electrolyte favours a proton insertion mechanism as opposed to the lithium ion insertion mechanism which is observed with the LiOH electrolyte [8, 9].

4 Conclusions

The present work has investigated Zn–MnO_2 cells using Li_2SO_4 as an electrolyte. The key electrochemical process involved in the Li_2SO_4 containing cell appears to be proton insertion, being similar to the well known alkaline manganese cell using KOH as an electrolyte. However, the addition of bismuth oxide to the MnO_2 does result in rechargeable behaviour. This is in marked contrast to MnO_2 cells using LiOH as an electrolyte, where the key electrochemical process involves lithium ion insertion into the MnO_2 lattice. Such cells exhibited multiple rechargeability even without any additives such as bismuth. The formation of lithium carbonate which acts as an over layer in LiOH electrolyte explains this difference. Bismuth additions help to suppress the formation of Mn_3O_4 during discharge. They also promote the formation of birnessite MnO_2 during charge. Although this is a non-rechargeable product it does help to stabilize the MnO_2 structure.

Acknowledgements The authors would like to thank the Australian Institute of Nuclear Science and Engineering (AINSE) for providing financial assistance (AINGRA Award 08048) for access to XRD facilities at ANSTO.

References

1. Linden D (1995) In: Linden D (ed) Handbook of batteries, 2nd edn. McGraw-Hill, New York
2. Ohzuku T, Kitagawa M, Hirai T (1989) J Electrochem Soc 136:3169
3. Ohzuku T, Kitagawa M, Hirai T (1990) J Electrochem Soc 137:40
4. Kordesch KV (1974) Manganese dioxide. Marcel Dekker, New York
5. Kozawa A, Yeager JF (1965) J Electrochem Soc 112:960
6. Donne SW, Lawrence GA, Swinkels DAJ (1997) J Electrochem Soc 144:2961
7. Yu LT (1997) J Electrochem Soc 144:802
8. Minakshi M, Singh P, Issa TB et al (2004) J Power Sources 130:254
9. Minakshi SP, Mitchell DRG (2007) J Electrochem Soc 154:A109
10. Sajdl B, Micka K, Krtil P (1995) Electrochim Acta 40:2005 and references listed therein
11. Wroblowa HS, Gupta N (1987) J Electroanal Chem 238:93
12. Wroblowa HS, Kummer JT, Yao YF (2004) EP Patent No. 0 146 201 A.
13. Im D, Manthiram A (2003) J Electrochem Soc 150:A68
14. Castledine CG, Conway BE (1995) J App Electrochem 25:707
15. Luo JY, Xia YY (2007) Adv Funct Mater 17:3877
16. Yang CC, Lin SJ (2002) J Power Sources 112:174
17. Minakshi M, Singh P, Issa TB et al (2007) Electrochim Acta 52:7007
18. Kannan AM, Bhavaraju S, Prado F et al (2002) J Electrochem Soc 149:A483
19. Minakshi M, Singh P, Issa TB et al (2004) 41st Proceedings of the power sources conference, Philadelphia
20. Seguin MK (1972) Am Mineral 57:511
21. Wu YT, Hu CC (2005) Electrochem Solid State Lett 8:A240